THE EFFECT OF WAKE THICKNESS ON THE ROLLING-UP PROCESS IN TWO DIMENSIONS*

H. Portnoy**
Department of Aeronautical Engineering,
Technion - Israel Institute of Technology,
Haifa, Israel.

Abstract

A numerical method is developed for calculating the flow field due to a two-dimensional distribution of vorticity over a given area. A distribution of vorticity over a long thin ellipse is then used to model the flow about the unrolled cross-section of a thick wake far downstream of the wing trailing-edge. The distribution is now allowed to distort under the action of its own induced velocity field, (which is calculated by the aforementioned numerical method), thus simulating roll-up of a wake with thickness. The influence of viscosity is neglected and two different span loadings are studied.

List of Symbols

A, A'	wake cross-sections at a general station x and at $x = 0$, respectively.
AR	aspect ratio of wing.
a, b, c	sides of triangular element divided by s - see Fig. 2.
C, C'	boundaries of cross-sections A and A', respectively.
C_L	wing lift coefficient.
K_n	$= \xi_n^* \Delta A_n^*$.
M	total number of triangular elements in wake cross-section.
N	number of different values of ξ_n^* .
n	number denoting a typical triangular element.
P	perimeter of S.
r_A, r_B, r_C	see Equation (13) and Fig. 2.
S	closed region with constant vorticity distribution.
s	wing semi-span.
t^*	dimensionless time. See Equation (4).
U	free stream velocity.
V_n, W_n	element influence functions. See Eqs. (14) and (15).
v, w	velocity components in the y and z directions, respectively.
w_I^*	$-w_I^*$ is the non-dimensionalised downwash calculated in the Treffz plane for an unrolled wake.
x, y, z	system of coordinates - see Fig. 1.
α, β, γ	see Eq. (13) and Fig. 2.
α_B, α_C	see Eq. (13).
β_A, β_C	see Eq. (13).
γ_A, γ_B	see Eq. (13).
ΔA_n	area of nth triangular element.
Δt^*	dimensionless time step in numerical integration.
$\Delta v_n^*, \Delta w_n^*$	contributions to v^* and w^* from nth triangular element.
ε	thickness ratio of elliptic wake cross-section.
ζ	$= y + iz$.
$\zeta_A, \zeta_B, \zeta_C$	ζ at corner A of nth element, etc.
θ	$= \cos^{-1} y^*$.
λ	$= \tan^{-1} (dz^*/dy^*)_{C'}$.
$\xi(x,y,z)$	vorticity distribution within A.
ξ_n	constant value of ξ in nth triangle.
ξ_s	constant value of ξ inside S.
$\omega(y)$	vorticity distribution within A'.
$( )^*$	denotes non-dimensional forms of variables defined in Eqs. (2)-(5) and (12).

* This research was supported in part by the Air Force Office of Scientific Research (AFSC), United States Air Force under Grant AFOSR 71-2045.

** Associate Professor.

I. Introduction

Many investigators have studied the rolling-up of the vortex wake behind a wing of finite span. The earliest step in this study was the work of Kaden[1] who found an analytical solution for the rolling-up with time of a semi-infinite, straight, two-dimensional vortex sheet. This solution must represent the situation very close to the edges of a finite-span vortex sheet of zero thickness, in two or three-dimensions, during the initial stage of the rolling-up process. An important result following from Kaden's work is that, from the very onset of rolling-up, due to the infinite velocity at the sheet edge, a spiral of near-axisymmetric form, with an infinite number of turns, is established at the edge. This is a consequence of the assumption of zero thickness for the sheet.

Westwater[2] considered a finite-span, zero-thickness wake resulting from an elliptically-loaded wing and assumed that the roll-up could be treated as a two-dimensional time-dependent process, where the configurations at successive stages in time represent successively further downstream sections of the wake, as fixed by the forward speed of the wing multiplied by the time. This approach is evidently suitable for wakes which roll up relatively slowly far behind the wing, such as are found with high-aspect-ratio, unswept wings. Westwater further simplified his calculations by replacing the continuous vortex sheet by a row of infinite line vortices. Clements and Maull[3] have recently used this technique for non-elliptic span-loadings. Westwater's method is subject to certain numerical difficulties which have been the subject of a number of investigations. A particularly careful recent review and study of this matter is due to Moore[4], who develops a method for overcoming the problem.

The line-vortex method has been extended to cover three-dimensional effects, such as those of bound vorticity and the finite origin and streamwise curvature of the trailing vortices, by the use of the vortex-lattice procedure[5,6,7,8,9]. This leads to results applicable to low-aspect-ratio and swept wings.

Recently an early method of Betz[10] for approximately determining the fully-developed, rolled-up vortex structure has been developed and extended by a number of authors[11],[12],[13]. This method makes use of a number of conservation relationships between the core and the unrolled sheet (not all of which are exact) and seems to assume, implicitely, that the wake has no thickness.

The present work is an attempt to remove the unrealistic features of the various earlier models, namely zero wake thickness and vorticity concentrated on lines, by assuming that the wake vorticity is contained in a layer of finite thickness with some plausible cross-sectional shape. The wake flow is assumed to be two-dimensional and the rolling-up is studied via the time-dependent development of this model, exactly as in Westwater's work, so that we deal with a slow rolling-up taking place far behind the wing, once more. The introduction of vorticity distributed continuously throughout the wake cross-section enables us to obtain a more acceptable picture of the initial rolling up phase than the infinite spiral of Kaden[1].

Having selected an appropriate wake cross-section its area is divided into triangular elements within each of which the vorticity is assumed constant, and for which simple expressions giving the velocity field have been derived (see Section 3). The strength of the vorticity within each triangle is determined using two assumptions:

(1) The vorticity is constant through the wake thickness. This corresponds to an assumption that the transverse velocity profile within the wake is linear.

(2) The periphery of the wake is moving downwards with a velocity determined by spanwise position and wing spanwise loading, exactly as in ordinary wing-wake theory.

Assumption (1) can evidently be removed at the cost of increasing the number of triangular elements used.

Once the triangle strengths are found, the network of points defining the wake is allowed to distort with time under its self-induced velocity field, using Euler integration. During this process viscous dissipation is neglected, so that the vorticity inside each triangle remains constant, as will its area (due to continuity), even though the shape changes.

Examples of the initial roll-up phase have been calculated for three wakes of different thicknesses and elliptic cross-sections, subjected to uniform downwash (corresponding to elliptic spanwise loading). For the thickest of the three (thickness ratio .06) the calculation was carried on until about 80% of the original wake vorticity was rolled up. Details and results are given in Sections 5 and 7.

In Section 6 an example of an elliptic cross-sectioned wake of thickness ratio .06, subject to non-uniform downwash, (i.e. non-elliptic loading) is given. The loading chosen is one of the examples calculated by Clements and Maull[3] which yields two separate roll-up regions. The results are discussed in Section 7 and the effects of wake thickness on the secondary roll-up are shown to be very important.

II. The Mathematical Model

The mathematical model of the wake and the notation are illustrated in Fig. 1.

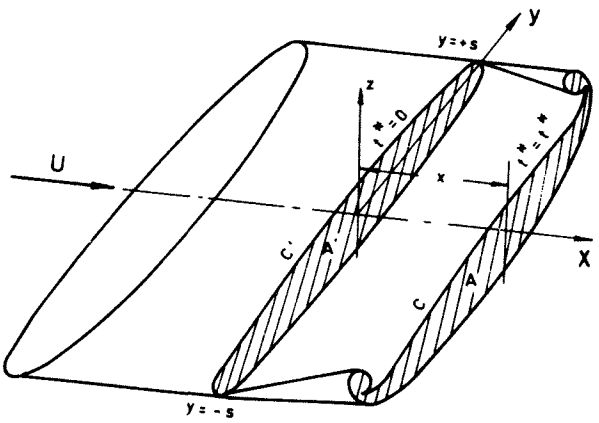

FIG. 1 WAKE CROSS-SECTIONS & SYSTEM OF AXES

The unrolled wake cross-section A', whose boundary is denoted by C', stretches between $y = -s$ and $y = +s$ in the plane $x = 0$. At subsequent stations $x = x$, the boundary is denoted by C and the wake has a rolled up form of cross-section A with vorticity distribution $\xi(x,y,z)$ determined by the original configuration of the wake cross-section, the original vorticity distribution within it, $\xi(0,y,z)$, and the elapsed time x/U. It is assumed that

$$\xi(0,y,z) = \omega(y) \qquad (1)$$

corresponding to a linear variation with z of the velocity, v, within the initial wake section, if the wake is assumed thin.

We define dimensionless coordinates

$$y^* = \frac{y}{s} \; ; \quad z^* = \frac{z}{s} \qquad (2)$$

and since a typical velocity of the flow in the wake cross-sectional plane is $2UC_L/\pi.AR$, we also define dimensionless velocity components, time and vorticity by

$$v^* = \frac{\pi AR.v}{2UC_L} \; ; \quad w^* = \frac{\pi AR.w}{2UC_L} \; , \qquad (3)$$

$$t^* = \frac{2C_L x}{\pi.AR.s} \; , \qquad (4)$$

$$\omega^*(y^*) = \frac{\omega\,\pi.AR.s}{2UC_L} \; ; \quad \xi^*(t^*,y^*,z^*) = \frac{\xi\pi.AR.s}{2UC_L} \; . \qquad (5)$$

We assume that ω or ω^* is determined by the boundary conditions:

(a) $$w^* \cos\lambda - v^* \sin\lambda = w_I^*(y^*)\cos\lambda \qquad (6)$$

on C'

where $(dz^*/dy^*)_{C'} = \tan\lambda$, and

(b) $$\sqrt{v^{*2} + w^{*2}} \to 0 \quad \text{as} \quad \sqrt{y^{*2} + z^{*2}} \to \infty. \qquad (7)$$

$-w_I^*(y^*)$ is the non-dimensionalised downwash distribution in the Treffz plane as calculated from the usual unrolled thin-wake theory. For example, $w_I^* = -1$ for elliptic spanwise load distribution. It is readily shown that, in the general form, w_I^* is dependent on the form of the spanwise loading and y^* only (c.f. Reference 3).

It now follows that for a given initial wake cross-section and spanwise loading, the velocities v^* and w^* of a given fluid particle are functions of t^* only, so that the subsequent non-dimensional coordinates of the particles constituting the rolled wake are functions of t^* only, determined by the differential equations

$$\frac{dy^*}{dt^*} = v^* \quad ; \quad \frac{dz^*}{dt^*} = w^* \quad . \tag{8}$$

The equations (8) are integrated numerically step by step, starting from the initial configuration, using Euler integration.

It remains to determine the velocity field (v^*, w^*) due to the distribution ξ^* within C.

III. The Velocity Field

At any value of x, the two-dimensional velocity field, (v,w), is determined by integrating the effects of point vortices of strengths $\xi(x,y,z)\,dy\,dz$ over the area of the wake cross-section, A.

To facilitate the numerical calculations, A is divided into a finite number of small straight-sided triangular elements within each of which the value of ξ is assumed constant. We now find expressions for Δv_n^* and Δw_n^* due to a typical element of this kind for points outside its boundary, or approaching the boundary in a limiting sense. This enables us to calculate v^* and w^* for the assemblage of triangles at all the node points of the triangular mesh, including internal nodes of A, since such points may be regarded as being inside infinitesimal cavities excluded from all the adjacent triangles, and we calculate, in effect, the principal value of the velocity integral - which is precisely the required definition of this integral inside the vorticity distribution.

The velocity field outside any area S containing a constant vorticity distribution, ξ_s may be written

$$v - iw = \frac{-i\xi_s}{2\pi} \iint_S \frac{dy_1\,dz_1}{y+iz-y_1-iz_1} \quad . \tag{9}$$

Using Green's theorem, this may be converted to a line integral around P, the perimeter of S:

$$v - iw = \frac{i\zeta_s}{2\pi} \int_P \ell n(\zeta - y_1 - iz_1)\,dy_1 \tag{10}$$

where $\zeta = y + iz$.

If (10) is applied to a typical triangle of A, of area ΔA_n, vorticity distribution strength ξ_n and vertices defined by $\zeta_A, \zeta_B, \zeta_C$ (Fig.2), we obtain

$$\Delta v_n - i\Delta w_n = -\frac{-i\xi_n \Delta A_n}{\pi}\left\{\frac{\zeta - \zeta_A}{(\zeta_C-\zeta_A)(\zeta_B-\zeta_A)}\ell n(\zeta-\zeta_A) + \right.$$
$$\left. + \frac{\zeta - \zeta_B}{(\zeta_C-\zeta_B)(\zeta_A-\zeta_B)}\ell n(\zeta-\zeta_B) + \frac{\zeta - \zeta_C}{(\zeta_A-\zeta_C)(\zeta_B-\zeta_C)}\ell n(\zeta-\zeta_C)\right\}. \tag{11}$$

ζ_n and ΔA_n are both invariant with the motion for an infinitesimal triangle in incompressible flow, the product $\xi_n \Delta A_n$ being the circulation around the element.

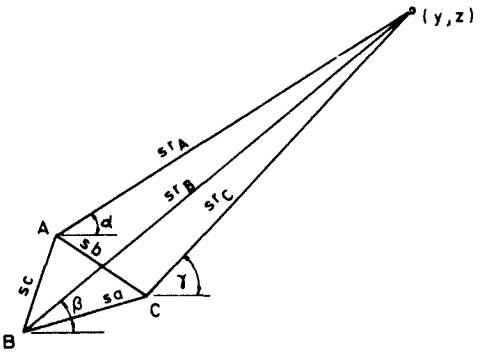

FIG.2 NOTATION FOR A TRIANGULAR ELEMENT & A FIELD POINT

If we now write $s^2 \Delta A_n^* = \Delta A_n$, then

$$\zeta_n \Delta A_n = \frac{2UsC_L}{\pi AR}\zeta_n^* \Delta A_n^* = \frac{2UsC_L}{\pi AR} K_n \tag{12}$$

and if (see Fig. 2)

$$\zeta - \zeta_A = sr_A e^{i\alpha} \; ; \; \zeta - \zeta_B = sr_B e^{i\beta} ; \; \zeta - \zeta_C = sr_C e^{i\gamma}$$
$$\zeta_B - \zeta_A = sce^{i\alpha_B} ; \; \zeta_C - \zeta_A = sbe^{i\alpha_C}$$
$$\zeta_C - \zeta_B = sae^{i\beta_C} ; \; \zeta_A - \zeta_B = sce^{i\beta_A}$$
$$\zeta_A - \zeta_C = sbe^{i\gamma_A} ; \; \zeta_B - \zeta_C = sae^{i\gamma_B} \tag{13}$$

we obtain from (11)

$$\Delta v_n^* = \frac{K_n}{\pi}\left\{\frac{r_A}{bc}[\sin(\alpha-\alpha_C-\alpha_B)\ell nr_A + \alpha\cos(\alpha-\alpha_C-\alpha_B)] + \right.$$
$$+ \frac{r_B}{ca}[\sin(\beta-\beta_C-\beta_A)\ell nr_B + \beta\cos(\beta-\beta_C-\beta_A)] +$$
$$\left. + \frac{r_C}{ab}[\sin(\gamma-\gamma_A-\gamma_B)\ell nr_C + \gamma\cos(\gamma-\gamma_A-\gamma_B)]\right\} =$$
$$= K_n V_n(y^*, z^*) \tag{14}$$

$$\Delta w_n^* = \frac{K_n}{\pi}\left\{\frac{r_A}{bc}[\cos(\alpha-\gamma_C-\alpha_B)\ell nr_A - \alpha\sin(\alpha-\alpha_C-\alpha_B)] + \right.$$
$$+ \frac{r_B}{ca}[\cos(\beta-\beta_C-\beta_A)\ell nr_B - \beta\sin(\beta-\beta_C-\beta_A)] +$$
$$\left. + \frac{r_e}{ab}[\cos(\gamma-\gamma_A-\gamma_B)\ell nr_C - \gamma\sin(\gamma-\gamma_A-\gamma_B)]\right\} =$$
$$= K_n W_n(y^*, z^*) \; . \tag{15}$$

Hence we have the approximations

$$v^* \approx \sum_{n=1}^{M} K_n V_n(y^*, z^*) \qquad (16)$$

$$w^* \approx \sum_{n=1}^{M} K_n W_n(y^*, z^*) \qquad (17)$$

IV. The Numerical Procedure

Because of the spanwise symmetry of the initial cross-section, A', and the assumption (1), the M values of K_n are dependent on a smaller number of values of ξ_n^*, say N. The boundary condition (6) is now applied at N suitable node points on the initial boundary A' (excluding the tip points), using the expressions (16) and (17), with unknown coefficients, $K_n = \xi_n^* A_n^*$, thus yielding N linear equations for the ξ_n^* and hence the K_n. The equations (16) and (17) may now be used to evaluate v^* and w^* at all values of t^*, once the dimensionless coordinates of the triangles are known. These are found step by step by numerical integration of the equations (8) forward in time t^*, starting with the known initial set of triangles within A'. The development of the wake roll-up is thus calculated step by step. The y^* coordinate of the "centroid" of vorticity of one half of the wake is calculated at each step. This should remain constant[10] and provides an accuracy check.

V. The Wake of Elliptic Cross-Section Subject to Uniform Downwash

In this case the equation of C' is

$$z^* = \pm\sqrt{1 - y^{*2}} \qquad (18)$$

and

$$w_I^* = -1. \qquad (19)$$

Also

$$\tan\lambda = \pm \frac{\varepsilon y^*}{\sqrt{1 - y^{*2}}} \qquad (20)$$

The cross-section A' was divided into triangular elements as shown in Figure 3. It was found necessary to concentrate the triangles near the tips. This was done as follows: Firstly, a basic set of spanwise stations was established by using an even number of equal divisions of the eccentric angle coordinate

$$\theta = \cos^{-1} y^* \qquad (21)$$

across the span. Next, the segments at the tips themselves were further subdivided into two equal θ intervals and all resulting divisions were then again subdivided into two for a specified number of the segments, starting from the tips and moving inboard. Using the horizontal diameter of the ellipse as another division line, triangles may then be filled in as shown in Figure 3. ξ_n^* is taken as constant over the four triangles lying between any two vertical lines (at the tip - over two triangles) and the same value is taken for the symmetrically placed group on the other half wake. In the illustration, the spanwise subdivision is 8 + 2 + 6, (8 basic divisions + 2 extra at tips + 6 additional subdivisions from tips, inwards), the number of triangles is 60 and the number of different values of ξ_n^* is 8. The points for applying the boundary condition are shown circled.

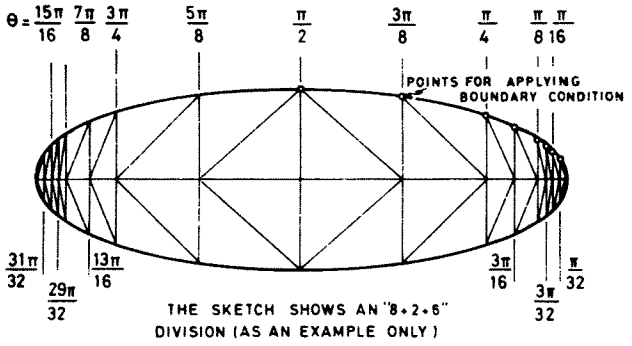

FIG. 3 LAYOUT OF ELEMENTS IN ELLIPTIC WAKE

An analytic solution exists for the downward moving elliptic cylinder, which corresponds to the flow at $t^* = 0$. The flow calculated by the present method at $t^* = 0$ was compared to this for the three cases considered namely, ε = 0.4, 0.5 and .06. In all these cases, a subdivision of 40 + 2 + 8 spanwise gave results for surface velocity, total amount of vorticity in one half wake and spanwise position of centroid, which were considered to compare adequately with the theoretical values and this distribution of points was also found to be just adequate for describing the spiral structure of the core up to the times reached in the calculations of the initial roll-up. During the initial roll-up, the centroid position spanwise remained constant to a high degree of accuracy for the range covered (change not more than 1 part in 780). The total times covered in the initial roll-up calculations were t^* = .0128, .0160 and .0192 for the thickness ratios 0.4, 0.5 and 0.6, respectively.

The appearance of the tip region is shown for various stages of this initial roll-up in Figures 4a and 4b for ε = .06 It should be noted, that to clarify the inner detail of the spiral, the vertical scale has been exaggerated in these figures.

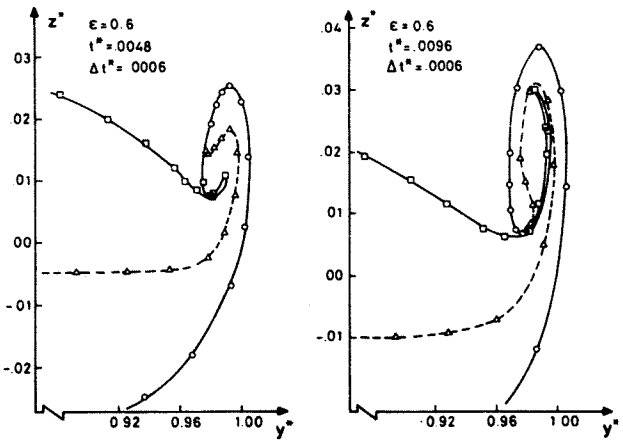

FIG. 4a INITIAL DEVELOPMENT OF VORTEX-ELLIPTIC LOADING

For ε = 0.6 extended calculations were carried out, reaching values of t^* beyond 1.3. However, for the later stages of the calculation, the accuracy, as indicated by the centroid position, began to deteriorate seriously, so results are

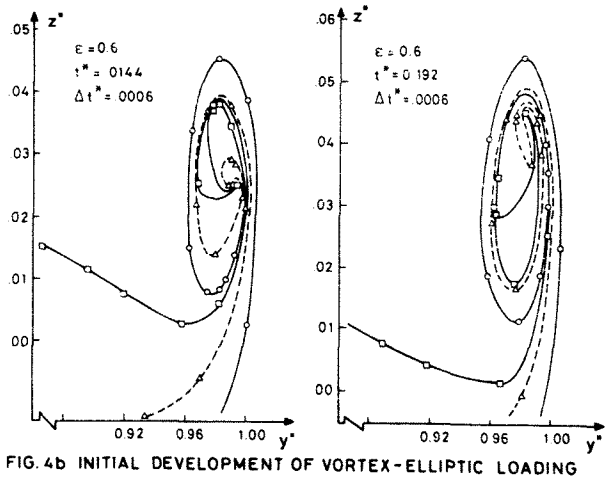

FIG. 4b INITIAL DEVELOPMENT OF VORTEX-ELLIPTIC LOADING

only given here up to $t^* = 1.3$. This matter is discussed further in Section 7. In order to carry out this calculation it was necessary to employ a 40 + 2 + 40 division of the wake. It was also found possible (and necessary) to increase Δt^* in stages during the calculation. Thus, the calculation was performed with Δt^* equal to .0006 up to $t^* = .0192$, with Δt^* equal to .0012 from .0192 till .0576, Δt^* equal to .0024 on till .1344, Δt^* equal to .0048 up till .9024, and Δt^* equal to .00305 from then until 1.000 (during this stage Δt^* was adjusted to reach 1.000 in 32 steps). After $t^* = 1.000$, $\Delta t^* = .00625$ was used.

Results of this calculation are shown in Figs. 5a and 5b and in Fig. 6 a graph of the fraction of vorticity rolled-up at time t^* is given for all the calculations of this Section in comparison with the results of Moore[4] and Kaden[1]. A discussion appears in Section 7.

VI. Wake of Elliptic Cross-Section Subject to a Certain Non-Uniform Downwash Distribution

In reference 3, Clements and Maull examine a number of non-elliptic span loadings (non-uniform downwash distributions) by the point vortex method. For several of them it was found that a considerable portion of the vorticity rolled-up into a second, inboard, vortex in addition to the tip vortex, so that the tip vortices were weaker than those of the elliptic distribution for the same C_L; although a certain penalty in induced drag, naturally, has to be paid.

One of the distributions is, in the notation of reference 3 (with a correction to a printing error in the coefficient on the right hand side):

$$\Gamma' = \frac{2}{\pi}(\sin\theta + c \sin 5\theta); \quad \delta = 10\% \qquad (22)$$

An extended calculation was carried out by the present technique for an $\varepsilon = .06$ elliptic-cross-sectioned wake, subject to the far-field downwash produced by the loading (22), with the object of determining if the inboard vortex developed in the same way.

Equations (18) and (20), with $\varepsilon = .06$, still apply in this example, but now the far-field downwash is

$$-W_I^* = +1 + \frac{\sqrt{2}}{10}\frac{\sin 5\theta}{\sin\theta} = +1 + \frac{\sqrt{2}}{10}(1 - 12y^{*2} + 16y^{*4}). \qquad (23)$$

Results of this calculation are shown in Figs. 7a, 7b, and 7c and a discussion appears in the next Section.

VII Results and Discussion

For the elliptic-loading calculation the time step Δt^* was found to be a very critical parameter in the initial stages of the calculation. Too small a value caused chaotic motion to appear after a large number of steps had been taken to cover the initial period of high distortion at the wake tip. On the other hand, too large a Δt^* led to incorrect wake shapes which were not substantiated on reduction of the time step. It was found that for each thickness ratio of the wake cross-section it was possible to find a value which avoided these extremes over the first 32 steps. For $\varepsilon = .04$, the appropriate Δt^* for the first 32 steps was .0004, for $\varepsilon = .05$ the value was .0005 and, for $\varepsilon = .06$, the value was .0006. The value found for $\varepsilon = .06$ was found to work well for the non-elliptic loading case too, which is not unexpected, since the initial rapid tip distortion should be fairly independent of the form of the span loading.

For extending the calculation with $\varepsilon = .06$, the time step was increased as described earlier in Section 5. This process was checked from time to time by covering a certain range both with the original and with the increased time step and seeing if the results for the wake form tallied well enough. This was always found to be so with the scheme described, although the vortex center-

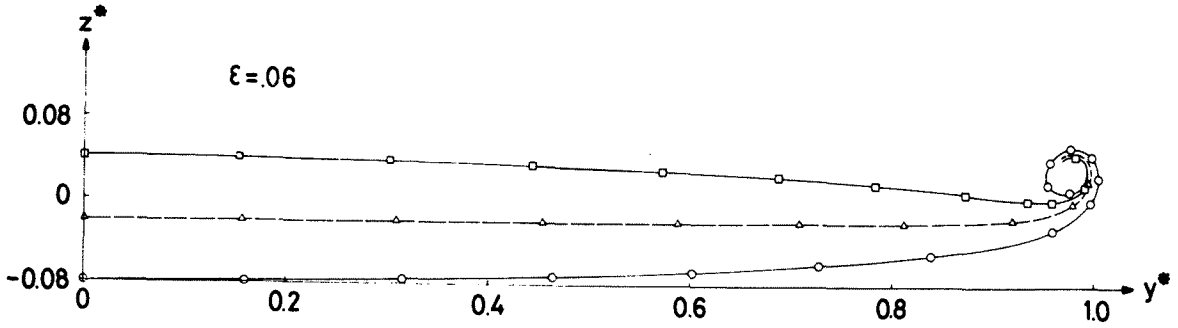

FIG. 5a CONFIGURATION AT $t^*=0.01920$ - ELLIPTIC LOADING

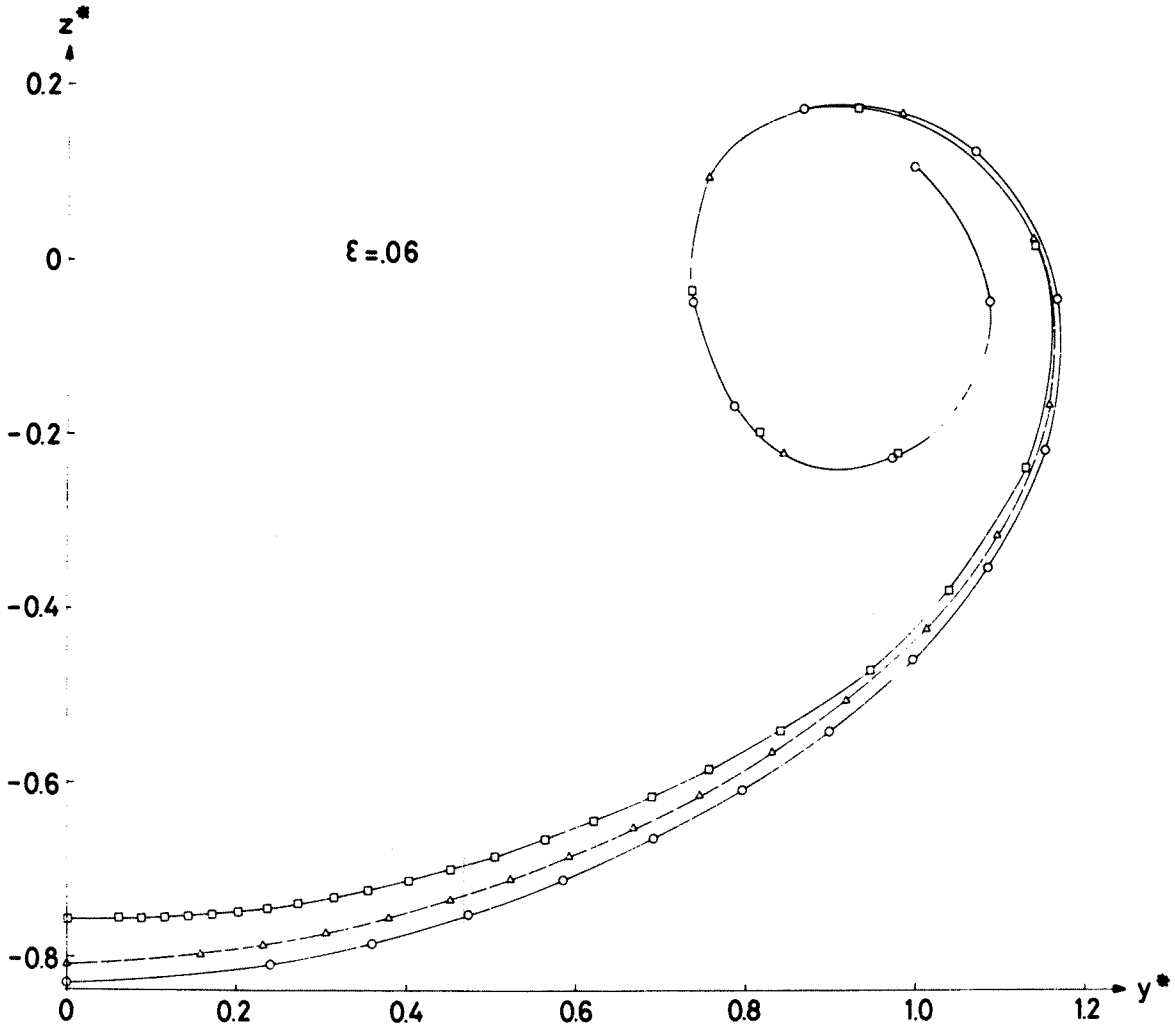

FIG. 5b CONFIGURATION AT t^*= 0.99999 - ELLIPTIC LOADING

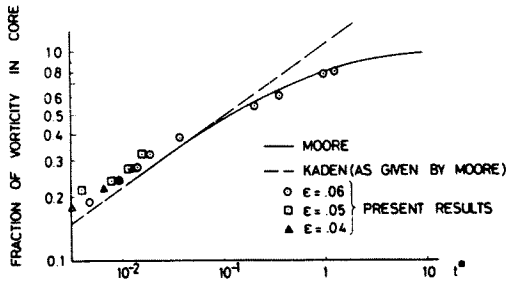

FIG. 6 FRACTION OF VORTICITY ROLLED UP AT t^*-ELLIPTIC LOADING

of-gravity position worsened slightly faster with the bigger time steps (see below), but not significantly so. The same time-step scheme was used for the non-elliptic load distribution without further check.

All the initial roll-up calculations were carried out with the 40 + 2 + 8 division, whereas the extended calculations for ε = .06, both with elliptic loading and with non-elliptic loading employed a 40 + 2 + 40 scheme. This was found to be necessary in order to define the outer spiral shape adequately.

At this point it is necessary to comment on the interpretation we give to the assemblage of points which results from the calculation at each step. Evidently, a smooth curve drawn through the points represents an approximation to the true wake shape, even though calculations of the velocity field and center-of-gravity position are based on a system of rectilinear triangles joining the points. As the difference between the two representations diverges, the accuracy of the velocity and center-of-gravity calculations worsens, so that the curvilinear shape is a less and less accurate representation of the true wake shape. However it is believed that the shape predicted is better than is indicated by the spanwise center-of-gravity position change which, for example, reaches 9.8% of the original value (outwards) at t^* = .99999, for the elliptic distribution (it is perhaps significant that the center-of-gravity drifts consistently outwards from the center line). This belief is reinforced by the comparison with Moore's[4] results given below. Complete verification of this thesis could of course, only be achieved by increasing the number of triangles to approximate closer to the spiral shape at all stages. Unfortunately this is impossible for practical reasons.

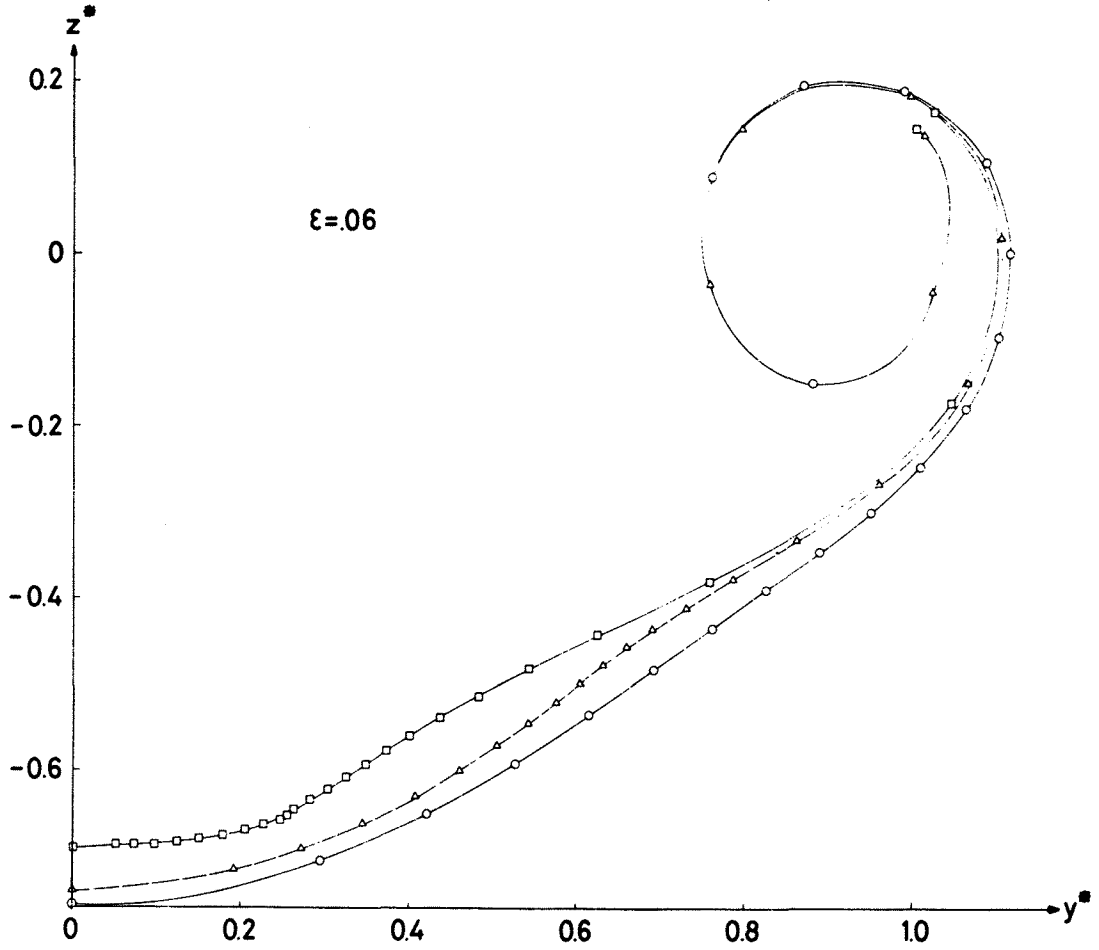

FIG. 7a CONFIGURATION AT $t^*=0.74879$
NON - ELLIPTIC LOADING

In the initial-roll-up stage the curvilinear and triangle representations are very close and the center-of-gravity remains constant to within one part in 780 or better, so we can have every confidence in the results. As the calculation is extended, however, the triangles in the center of the roll-up begin to overlap one another and may eventually change the cyclic order of their points. Under these conditions no acceptable smooth curve can be drawn and obviously the points have no real meaning. However, the method of calculation ensures that the vorticity is conserved under all circumstances, so that, as far as the outer spiral and other portions of the wake are concerned, we simply have a "condensation" of vorticity inside the spiral - rather analogous to Moore's technique[4], so that the shape of these outer portions is still accurate. Eventually, for t^* around unity, some of the outer triangles overlap too, due to the extreme stretching and shearing which has taken place in the increasingly curved mid-span portion of the wake; but by this time, the triangles involved are those with a very small fraction of the vorticity, (about 1% or less of the total), so that the affect on accuracy is not serious until beyond $t^* = 1.3$.

In Figs. 4a and 4b, stages in the initial roll-up for elliptic loading with $\varepsilon = .06$ are shown up to $t^* = .0192$. The corresponding pictures for $\varepsilon = .05$ (up to $t^* = .0160$) and .04 (up to $t^* = .0128$) are not shown, but they are very similar except in the matter of the number of turns in the spiral at a given t^*. Examination of the three sets of results yields the following conclusions concerning the effects of thickness ratio during the initial roll-up:

(1) Thickness has little effect on the amount of vorticity within the core at a given t^* (Fig.6).

(2) Thickness has almost no effect on the size of the rolled-up portion at a given t^*.

(3) Except in the very early stages, the rolled-up portion is of an approximately elliptic shape with height/width ratio about 0.8 for all three thicknesses.

(4) The turns of the spiral at a given t^* increase with decrease in ε, except, again, for the very-initial, ill-defined phase. Thus, for example, at $t^* = .012$ the number of turns is about 1.6 for $\varepsilon = .04$, 1.2 for $\varepsilon = .05$ and about 1 for $\varepsilon = .06$.

In comprehending these results, and those that follow, it may be observed that, if we take as typical values $C_L = 0.5$, AR = 8, then until t^*

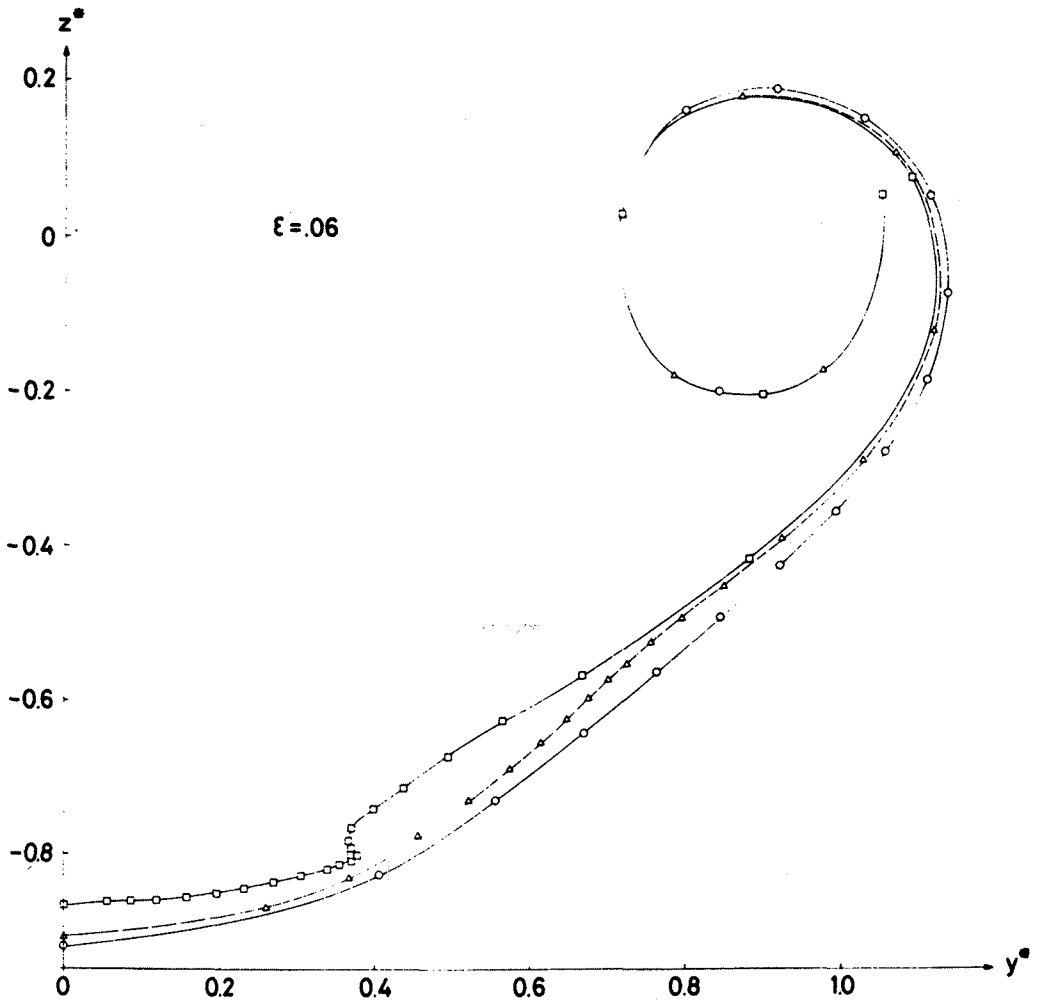

FIG. 7b CONFIGURATION AT t^*=0.99999
NON - ELLIPTIC LOADING

corresponds to $x/2s = 4\pi$, that is a downstream movement of about 12.5 span lengths.

In Fig. 5a an early phase ($t^* = .0192$) in the extended calculations for elliptic loading with $\varepsilon = .06$ is shown as a full half-span diagram with equal horizontal and vertical scales. This, in fact, represents the same state as the last picture of Fig. 4b. Despite the difference in the number of triangles used, there is no discernable difference between them. In Fig. 5b the form of this wake at $t^* = .99999$ is shown. This compares extremely well in size, shape and position with Moore's[4] spiral at $t^* = 1$, except that the main part of the spiral is very slightly shifted outboard.

In Fig. 6 the fraction of vorticity, rolled-up at time t^* is shown for all the present elliptic-loading calculations and these are seen to compare favourably with the results of Moore[4] and Kaden[1] (as quoted by Moore) - although the present results are consistently higher for $t^* < .1$ and are slightly lower for $t^* > .1$. It should be mentioned that, as far as was practical with the present set-up, Moore's[4] definition of the fraction rolled-up was adhered too. These results show that the two major effects of continuous vorticity in a thick wake which cannot be adequately modeled by point vortices - namely, thinning out of the vorticity by stretching and redistribution of vorticity per unit length of the wake cross-section by internal shearing - come effectively into play too late to affect the main parameters of the roll-up.

The form of the wake for the non-elliptic loading of equation (22) with $\varepsilon = .06$ is shown at three stages; $t^* = .74879$, $t^* = .99999$ and $t^* = 1.19997$ in Figs. 7a, 7b and 7c, respectively.

Although it appears at first as if the inboard vortex is going to develop just as in Reference 3, this process seems to be increasingly inhibited by the shearing within the wake thickness and the stretching of the bottom part of the layer near the crucial station so that, even though a "knob" of vorticity does develop, it is subsequently suppressed and a secondary hump forms further outboard. Calculations were carried out beyond the stage shown in Fig. 7c and show this process to develop further but the later results were deemed to be too inaccurate, so they are not shown. However, it is believed that the effects demonstrated are qualitatively correct and are not

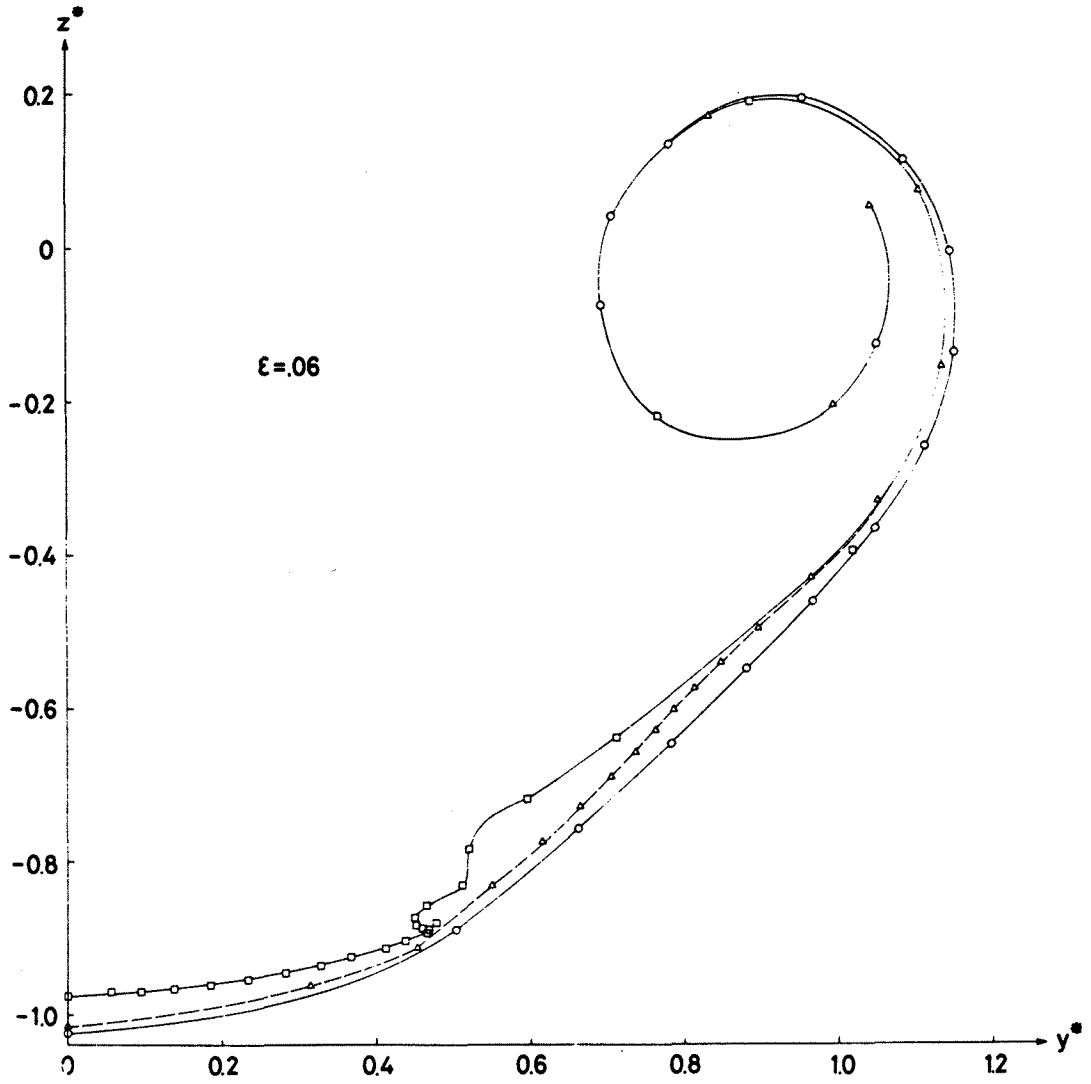

FIG. 7c CONFIGURATION AT $t^* = 1.19997$ NON - ELLIPTIC LOADING

simply numerical instabilities.

In conclusion, the relationship of the present two-dimensional thick-wake model to a real three-dimensional one, with axial velocity defect and viscous and turbulent decay, will be discussed. The effects of neglecting the three-dimensional effects of wing bound vorticity and the finite upstream extent of the trailing vortices have been described by Westwater[2], and will not be commented on further here. If the boundary-layer shed by the wing rolls-up with the wake, we would deduce that the velocity defect would have almost no effect on the present roll-up calculations, since the vorticity due to it is normal to the free stream direction and the wake is thin. There is, however, some experimental evidence that the slower moving fluid tends to gravitate towards the pressure sink at the vortex center, so causing the outer part of the spiral to be pushed outwards (see comment in reference 12 on the results of reference 14). Cliffone and Orloff[15] have shown that viscous and turbulence effects are fairly small for downstream distances of 25 to 45 span lengths behind the wing. This, coupled with the observed insensitivity of our ellptic-loading calculations to thickness ratio (diffusion would tend to effectively thicken the wake layer) and the fact that our calculations cover, perhaps, 16 or 17 span lengths at most, reinforces the conclusion that neglect of viscosity is justified in the present work.

Acknowledgments

The author wishes to thank Mr. B. Fortune, Mrs. R. Gordon and Mr. Y. Adler for help with the computer programming of this work.

References

1. Kaden, H., "Aufwicklung eines unstabilen Unstetigkeisfläche". Ing. Archiv., Vol. 2, pp. 140-168, May 1931 (English translation R.A.E. Library Translation No. 403).
2. Westwater, F.L., "The rolling up of the surface of discontinuity behind an aerofoil of finite span". British A.R.C. R & M 1692, 1935.
3. Clements, R.R., and Maull, D.J., "The rolling up of a trailing vortex sheet". The Aeronautical Journal, Vol. 77, No. 745, pp. 46-51, Jan. 1973.

4. Moore, D.W., " A numerical study of the roll-up of a finite vortex sheet". J. Fluid Mech., Vol. 63, Part 2, pp. 225-235, 1974.
5. Hacket, J.F., and Evans, M.R., "Vortex wakes behind high lift wings". Journal of Aircraft, Vol. 8, No. 5, pp. 334-340, 1971.
6. Hancock, G.J., and Butter, D.J., "A numerical method for calculating the trailing vortex system behind a swept wing at low speed". The Aeronautical Journal, Vol. 75, No. 728, pp.564-568, 1971.
7. Rom, J., Zorea, C. and Gordon, R., " On the calculation of non-linear aerodynamic characteristics and the near vortex wake". The 9th Congress of the ICAS, Haifa, Israel, ICAS Paper No. 74-27, August 1974.
8. Labrujere, Th., E., "A numerical method for the determination of the vortex sheet location behind a wing in incompressible flow". NLR TR 72091U, July 1972.
9. Maskew, B., "The calculation of potential flow aerodynamics characteristics of combined lifting surfaces with relaxed wakes". Hawker-Siddeley Aviation Ltd., (Brough) Aerodynamic Design Dept. Note YAD 3192, Sept. 1973.
10. Betz, A., "Verhalten von Wirbelsystemen". Z.A.M.M., Vol. 12, pp. 164-174, June 1932, (Also NACA TM 713, June 1933).
11. Donaldson, C. du P., Snedecker, R.S., and Sullivan, R.D., "A method of calculating aircraft wake velocity profiles and comparison with full-scale experimental measurements". AIAA Paper 74-39, Washington, D.C., 1974.
12. Jordan, P.F., "Structure of Betz vortex cores". Journal of Aircraft, Vol. 10, pp. 691-693, Nov. 1973.
13. Rossow, V.J., "On the inviscid rolled-up structure of lift-generated vortices". Journal of Aircraft, Vol.10, pp. 647-650, Nov. 1973.
14. Mason, W.H. and Marchman J.F. III, "Far-field structure of aircraft wake turbulence". Journal of Aircraft, Vol. 10, pp.86-92, Feb. 1973.
15. Cliffone, D.L. and Orloff, K.L., "Far-field wake-vortex characteristics of wings". Journal of Aircraft, Vol. 12, pp. 464-470, May 1975.